

D. LEŚNIAK\*

## WELDABILITY INVESTIGATIONS OF AlCuMg ALLOYS FOR EXTRUSION WELDING

### BADANIA ZGRZEWAŁNOŚCI STOPÓW AlCuMg PRZEZNACZONYCH DO WYCISKANIA NA MATRYCACH MOSTKOWYCH-KOMOROWYCH

The extrusion of hollow shapes from high strength aluminum alloys with the use of porthole dies encounters, in practice, great difficulties, mainly due to the poor weldability of these materials and the high forces needed to conduct the process. In the work, an original method and a special device are presented, which enable to determine the welding conditions of hard deformable aluminum alloys. The main advantage of the proposed method is that it simulates the conditions occurring in the welding chamber of the porthole dies. The weldability tests were performed for the 2024 alloy with extreme contents of Cu and Mg, in a wide range of welding temperatures and pressures. The microstructure and the seam welds' strength were also examined. The welding conditions for 2024 alloy, which allowed for obtaining high-quality seam welds were determined. The parameter describing the ability to weld was defined as the stress necessary for the welding to the yield stress ratio ( $\sigma_w/k$ ) and was determined for the analyzed alloys. The obtained welding stress values will be the basis for the porthole die design.

*Keywords:* weldability, AlCuMg alloys, extrusion, porthole dies

Wyciskanie kształtowników pustych z wysokowytrzymałych stopów aluminium z wykorzystaniem matryc mostkowych-komorowych napotyka w praktyce na poważne trudności, wynikające głównie ze słabej zgrzewalności tych materiałów i wysokich sił potrzebnych do przeprowadzenia procesu. W pracy przedstawiono oryginalną metodę i urządzenie, które umożliwiają określenie warunków zgrzewania trudno odkształcalnych stopów aluminium. Główną zaletą proponowanej metody jest to, że pozwala na odzwierciedlenie warunków zgrzewania, jakie panują w komorze zgrzewania matrycy mostkowej-komorowej. Próby zgrzewalności przeprowadzono dla stopu 2024 z graniczną zawartością Cu i Mg, w szerokim zakresie temperatur i nacisków jednostkowych zgrzewania. Badano strukturę i wytrzymałość zgrzewów. Określono warunki zgrzewania stopu 2024, które pozwoliły na otrzymanie wysokiej jakości połączenia. Zdefiniowano parametr opisujący zdolność do zgrzewania jako stosunek minimalnego naprężenia zgrzewającego (koniecznego do zgrzania) do naprężenia uplastyczniającego ( $\sigma_w/k$ ) i wyznaczono jego wartość dla analizowanych stopów. Uzyskane wartości naprężenia zgrzewającego będą podstawą do projektowania matryc mostkowych-komorowych.

## 1. Introduction

One of the most common techniques of producing hollow shapes from aluminum and its alloys is the technology based on hot extrusion with the application of porthole dies. As we analyze the course of the process, we learn that the heated extruded billet is split on a die's bridge into separate streams. These streams of metal that flow through the inlet ports join in a welding chamber surrounding the mandrel and next come into the die clearance, forming a hollow shape. In this way, we obtain products with longitudinal welds (seam welds), whose number corresponds to the construction of the die bridge. The welds, in the case of an incorrect selection

of the welding conditions, can be the cause of a lowered material strength in the product.

The described method of extrusion through porthole dies, called the welding extrusion, is commonly applied in the production of hollow sections from easy to deform aluminum alloys from the series 1xxx, 3xxx and 6xxx, which demonstrate good weldability. As for now, it is known from the practice that those aluminum alloys, which contain copper, especially durals (AlCuMg alloys), due to the poor weldability and the high resistance to deformation, cannot undergo the process of extrusion welding. The manufacturing of hollow shapes from aluminum alloys with poor deformability and weldability, based on hot extrusion through conventional dies, with

\* AGH UNIVERSITY OF SCIENCE AND TECHNOLOGY, FACULTY OF NONFERROUS METALS, 30-059 KRAKÓW, 30 MICKIEWICZA AV., POLAND

the punching of the billet, has, in turn, low efficiency and also, it significantly limits the assortment of the produced sections. The present possibilities of extruding products from AlCuMg alloys are thus limited to solid profiles of relatively simple shapes, or round pipes, with thick walls and low dimensional accuracy.

Modern construction, transport and a range of other branches of industry, feel a great necessity of applying light sections of high strength. That is why an important issue is to overcome the difficulties, which make it impossible to perform extrusion welding on these products. The key is a proper selection of the welding conditions, which must be provided in the welding chamber, in order for the product to meet the assumed strength requirements. Taking into account the theoretical premises, we can state that even the most difficult aluminum alloys can be welded, providing that we apply a high enough welding temperature, a high unit pressure, which works for a possibly long time, and a high non-dilatational strain in the welding area [1-2]. Obtaining the high-quality welds in these alloys can be stimulated by the results of the extrusion tests performed at very high homologous temperatures [3, 4], making it possible to significantly lower the extrusion force, with the provision of a high temperature of the material in the deformation area.

## 2. New method for weldability testing

In order to effectively design the tools and parameters of the extrusion welding process of high-strength aluminum alloys, it is necessary to perform a test, which investigates the influence of the basic parameters deciding about the weldability of the given alloy. The so far known methods of evaluating the weldability of aluminum alloys do not fully reflect the welding conditions during extrusion through porthole dies, and thus the obtained results are difficult to be used in practice. In the works [5-6], authors applied a special bridge die enabling extrusion of the three flat sections with the welds. Weldability investigations were performed for different aluminium alloys such as 6063, 6082, 6151 and 5052. The disadvantage of this method of the weldability assessment was that it does not allow for unambiguous determination of unit welding pressure in the welding

chamber, ensuring the good quality welds. Other methods of weldability testing [7-9] are based on welding two materials heated up by hot working, during which comes to increasing top surfaces of the joined materials. There are no such weldability tests during which one can simultaneously control the temperature, the unit pressure, the welding time and the degree of deformation in the welding area. A serious problem is maintaining the conditions of joining the metal with no access of air, which oxidizes the surface of the welded metal streams.

Coming from the nature of extrusion welding, where the cut apart metal streams before welding do not have contact with air, a new original device was proposed (Fig. 1, [10]), which allows for a reflection of the welding conditions in the welding chamber of a porthole die. The advantage of the invented method is the possibility of obtaining high quality welds, due to joining clean, non-oxidized surfaces, obtained in the process of hot plastic shearing performed directly before the welding process. Fig. 1 (left) shows the testing weldability device (upper and lower cutting punch) – before (Fig. 1a) and after (Fig. 1b) the process of plastic samples shearing.

The essence of the patented method of weldability testing [11] comes down to a special test of shearing of the given alloy's samples at the welding temperature and with the properly selected force of axial pressure, adequate to the determined unit welding pressure. By welding the samples obtained at different welding conditions, one can determine the desired unit pressure and the welding temperature, which guarantee a high strength of the weld.

The method consists in submitting two initial materials, upper  $m1$  and lower  $m2$ , first to hot shearing with the force  $F_s$ , and next to the force of axial pressure, which increases the compressive stresses in the formed welds (Fig. 1, right). The required forces of axial pressure are determined with the use of force  $F_w$ , necessary for cold cutting of auxiliary disks from arbitrarily selected materials  $m3$ , but with a strictly determined thickness.

Fig. 2 (right) shows the distribution of compressive stresses affecting the formed welds, as a result of the cold cutting force  $F_w$  of auxiliary disks at the final stage of the weldability test, which, at the same time, constitutes the force of axial pressure  $F_d$  (Fig. 2, left).

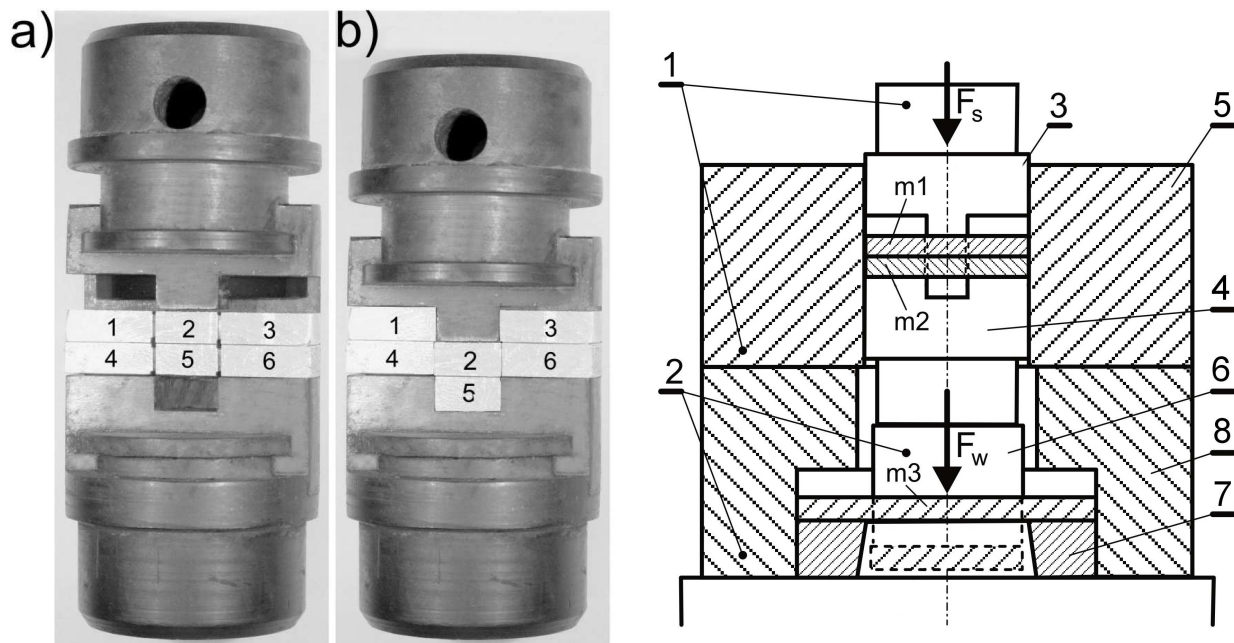


Fig. 1. Device for testing the weldability of aluminum alloys - main tools (left) and axial section (right) (a) before shearing, (b) after shearing and welding (1) main tool subassembly (2) auxiliary tool subassembly (3) upper cutting punch (4) lower cutting punch (5) container (6) blanking punch (7) cutting board (8) casing

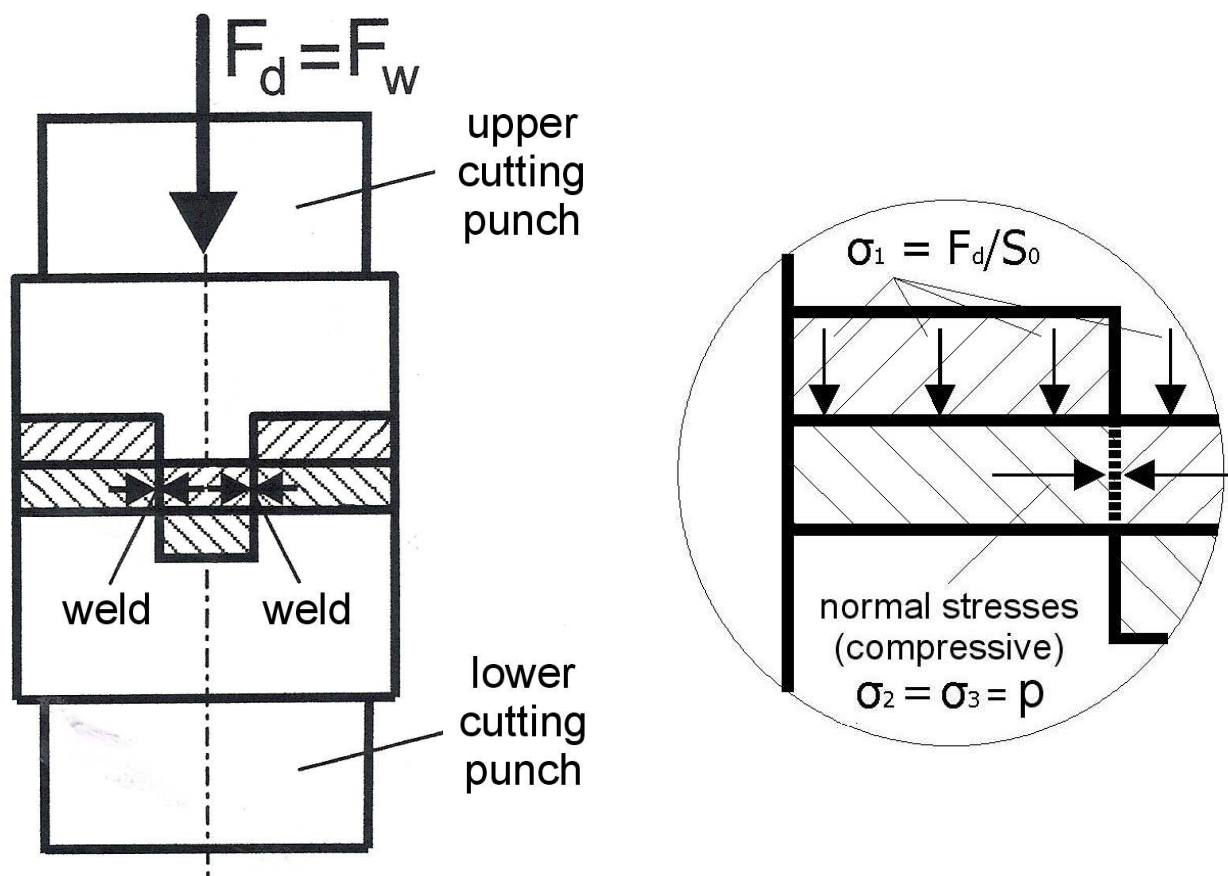


Fig. 2. Force of axial pressure  $F_d$  at final stage of weldability test (left) and distribution of compressive stresses affecting the created welds (right)

Thus, with the thickness of the auxiliary disks one can control the value of the force of axial pressure  $F_d$ . Knowing the dimensions and the area of the welded sample  $S_0$  (affected by force  $F_d$ ), one can determine the value of the compressive stress  $\sigma_1 = F_d/S_0$ . By simultaneous knowing of the flow stress value of the material  $k$  at the welding temperature, we can determine the value of normal compressive stresses  $p$  in the formed welds (unit pressure of welding) – formula (1.1a) and the mean stress value  $\sigma_m$  – formula (1.3).

Applying the known dependences of the theory of plasticity (1.1) and (1.2), we determined the formula for mean stress  $\sigma_m$  in the welding area (1.3), which ultimately includes the compressive stress  $\sigma_1$  (originating from the force of axial pressure  $F_d$ ), as well as the flow stress  $k$ .

$$\beta k = \sigma_1 - \sigma_3 \tag{1}$$

where:  $\beta$  – coefficient dependent on the indirect principal stress ( $\beta=1-1.15$ )

$k$  – flow stress

$\sigma_1, \sigma_2$  i  $\sigma_3$  – principal stresses (compressive)

as  $\sigma_2 = \sigma_3$  thus  $\beta = 1$ , and:

$$\sigma_3 = \sigma_1 - k \tag{1a}$$

$$\sigma_m = (\sigma_1 + \sigma_2 + \sigma_3)/3 \tag{2}$$

where:  $\sigma_m$  – mean stress

as  $\sigma_2 = \sigma_3$  thus:

$$\sigma_m = [\sigma_1 + 2(\sigma_1 - k)]/3 = \sigma_1 - 2k/3 \tag{3}$$

### 3. Material characterization

Weldability tests with the use of the method proposed above were performed for alloy 2024, with the

border contents of main alloy additions that are Cu and Mg (Table 1-2). In graphs, the alloys with the lowest and highest permissible content of Cu and Mg are to be called 2024 min and 2024 max respectively.

In order to determine the flow stress values for the border alloys at the welding temperatures (430, 500 and 530°C), high temperature compression tests of cylindrical samples ( $\varnothing 6 \times 8$  mm) were also performed, the latter produced on a special testing machine "Instron" (Fig. 3a), equipped with a protective atmosphere (argon) heat chamber and a system of measuring the temperature and force of the deformed samples. The appropriate lubrication of the surface of the major samples was applied for minimizing the friction. The flow stress curves  $k$  in the function of temperature, obtained for alloy 2024 with border contents of Cu and Mg, are presented in Fig. 3b.

TABLE 1

Chemical composition of 2024 alloy with the lowest permissible content of Cu and Mg, in wt. %

Element	Cu	Mg	Mn	Si	Fe	Zn	Ti
Weight %	3.56	1.23	0.90	0.06	0.12	0.028	0.03

TABLE 2

Chemical composition of 2024 alloy with the highest permissible content of Cu and Mg, in wt. %

Element	Cu	Mg	Mn	Si	Fe	Zn	Ti
Weight %	4.90	1.77	0.89	0.06	0.12	0.028	0.03

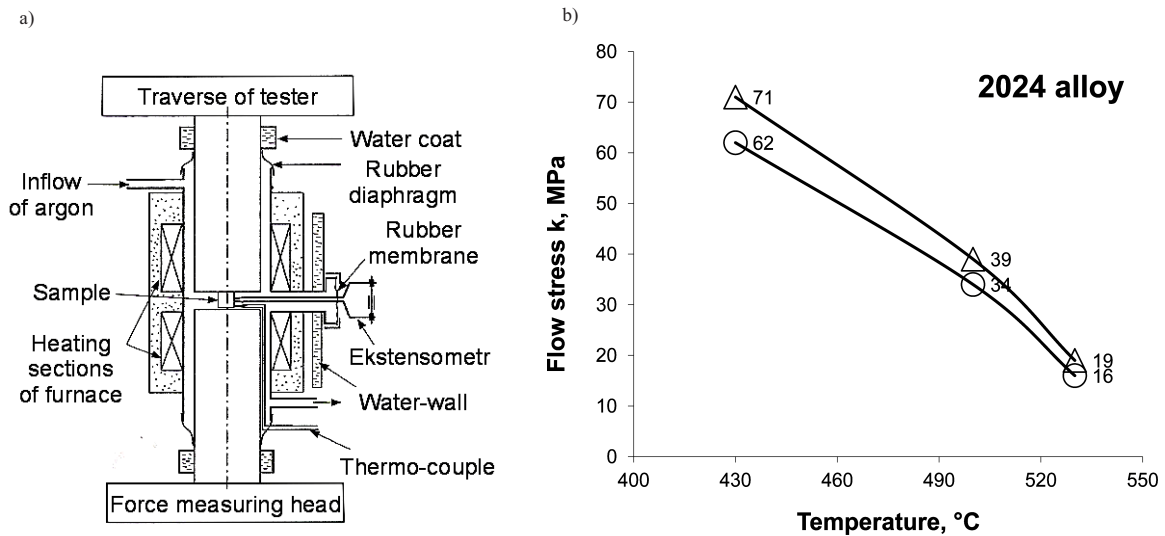


Fig. 3. Extrusion tests on alloy 2024 with border Cu and Mg content, for changing temperatures – 430, 500 and 530°C (deformation rate  $\dot{\epsilon} = 10^{-1} \text{ s}^{-1}$ ) (a) device scheme (b) dependence of flow stress  $k$  on deformation temperature



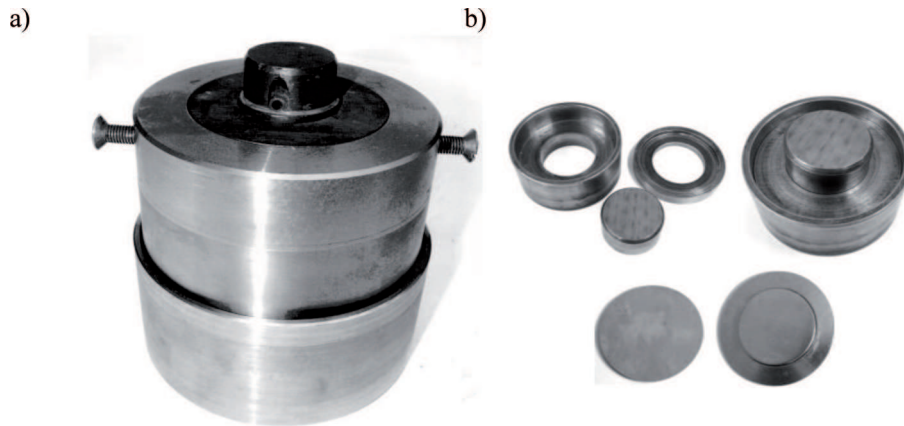


Fig. 4. Tools for weldability tests of aluminum alloys (a) complete tool set, (b) blanking punch, cutting board and sheared auxiliary disks

#### 4. Weldability investigations

The weldability tests were performed on a testing machine 100 kN (equipped with a measuring system of force and stroke), with the use of the proposed method and device. Fig. 4a shows a complete set of tools, that is a subassembly mounted directly on the auxiliary subassembly. Fig. 4b presents the elements of auxiliary subassembly together with the cold cut auxiliary disks.

Before the initialization of the tests, the auxiliary subassembly was placed on the testing machine – each time, 3 auxiliary disks were used, with the thickness of 1.5 mm (aluminium alloy 5754), which allowed for the obtaining of the shear force  $F_w$  equaling the force of axial pressure  $F_d$  at the level of 80 kN. Knowing the dimensions ( $40 \times 10 \times 5$  mm) and the area  $S_0$  ( $400 \text{ mm}^2$ ) of the welded sample affected by force  $F_d$  (80 kN), the value of the compressive stress  $\sigma_1 = F_d/S_0$  (200 MPa) was determined.

The main tool subassembly together with two identical samples, cubicoidal in shape, was heated in a furnace up to the desired temperature (430, 500 and  $530^\circ\text{C}$ ) for about 2 hours. The heated main subassembly was placed on the auxiliary subassembly, already located on the testing machine, and the weldability test was initialized. The deformation rate in the weldability tests equaled  $\dot{\epsilon} = 10^{-1} \text{ s}^{-1}$ , which corresponds to the deformation rate in the extrusion process of hard deformable aluminium alloys. Both the temperature of the material heating up to the weldability test and the temperature of the material during the weldability test were controlled with the use of thermocouple-sensors (type K, 1 mm thick), and recorded with the use of an Almemo 2690 recorder and the AMR Control 5.13 software.

Fig. 5 shows the recorded temperature of the welded alloy 2024, as well as the recorded shear force  $F_s$  and the force of axial pressure  $F_d$  in the function of the welding

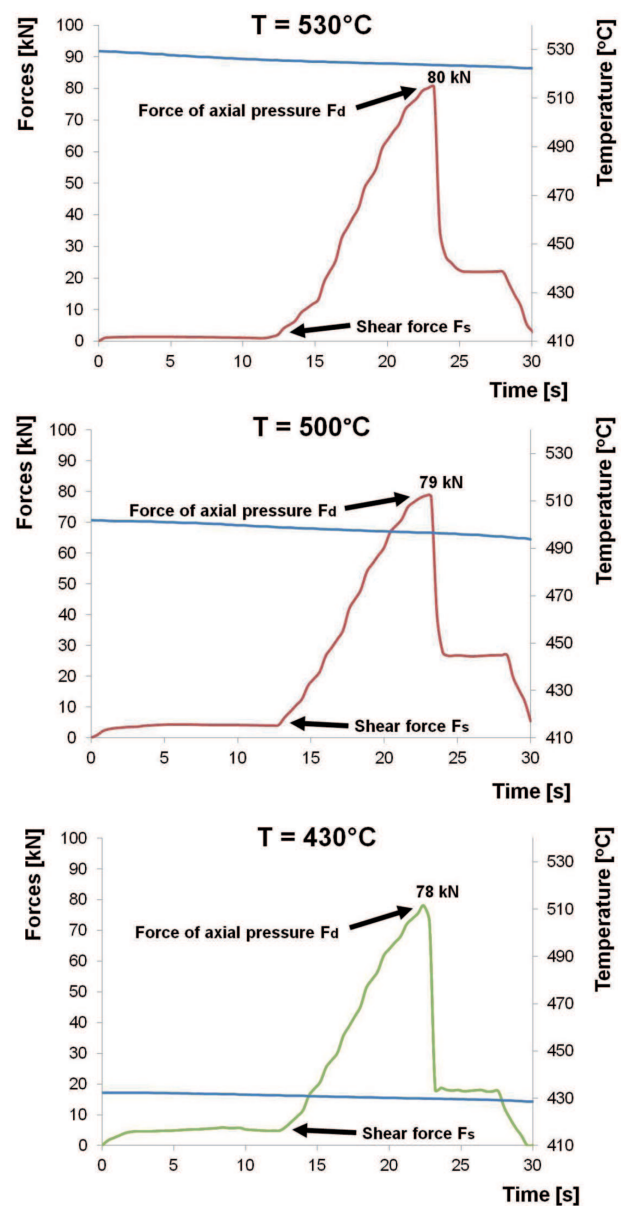


Fig. 5. Shearing force  $F_s$ , force of axial pressure  $F_d$  and welding temperature of material in the function of time for alloy 2024 heated up to different temperatures

test duration time. At the first stage of the weldability test, plastic shearing of the samples occurred, with a low force  $F_s$ , and next, in the process, the force rapidly increased, due to the cutting of auxiliary disks, to the moment of reaching the maximum, corresponding to the force of axial pressure  $F_d$ . As we always used identical disks, force  $F_d$ , in the tests performed at different temperatures, was almost identical and equaled approximately 80 kN. As is shown in Fig. 5, the temperature of welded material during weldability test practically remained at the same level.

### 5. Structure and Mechanical Properties of Pressure Welds

The samples with the welds formed in the weldability test, were submitted to structural and mechanical property examinations. Figs 6-7 show the microstructures of the samples welded at different temperatures – 430, 500 and 530°C – for alloy 2024 with border contents of Cu and Mg. The structures with increased magnifications concern the joining area.

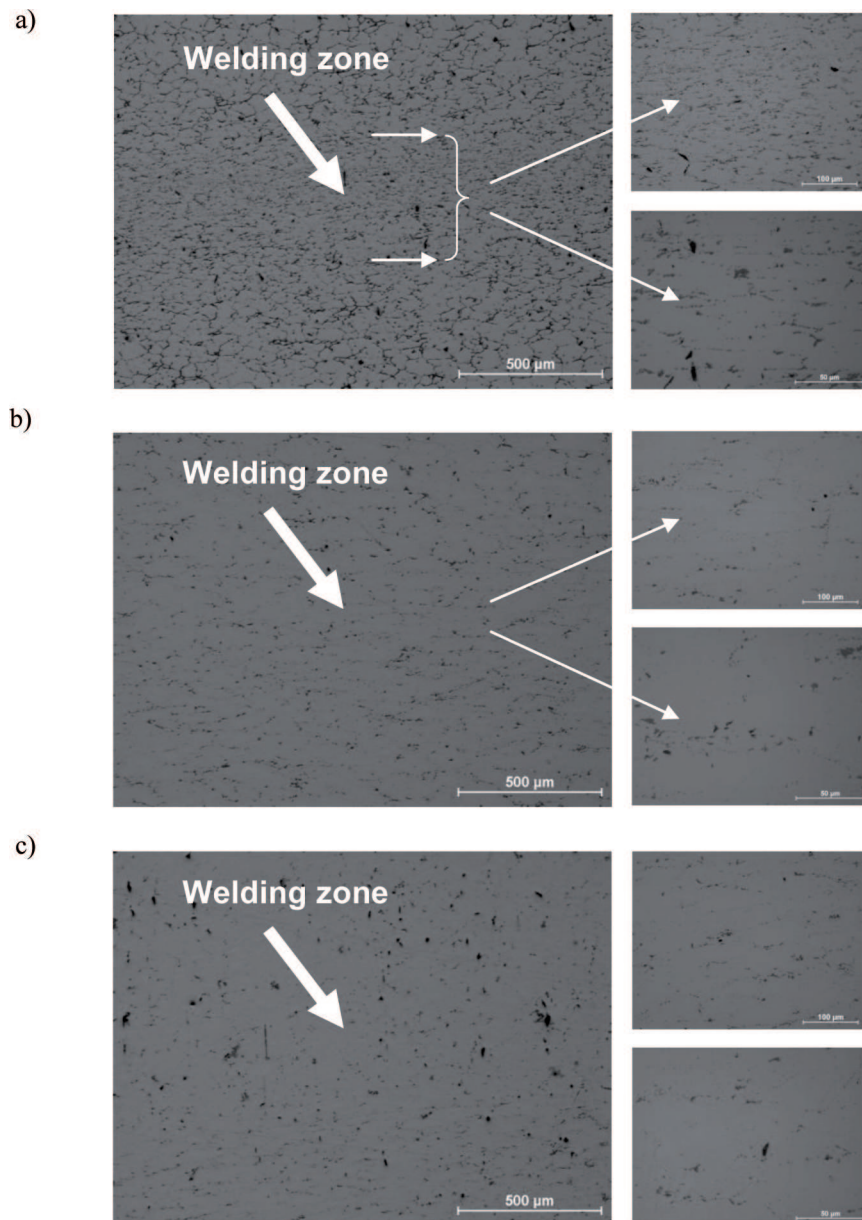


Fig. 6. Structures of the welded samples of alloy 2024 with the lowest permissible content of Cu and Mg for different welding temperature (a) T = 430°C (b) T = 500°C (c) T = 530°C

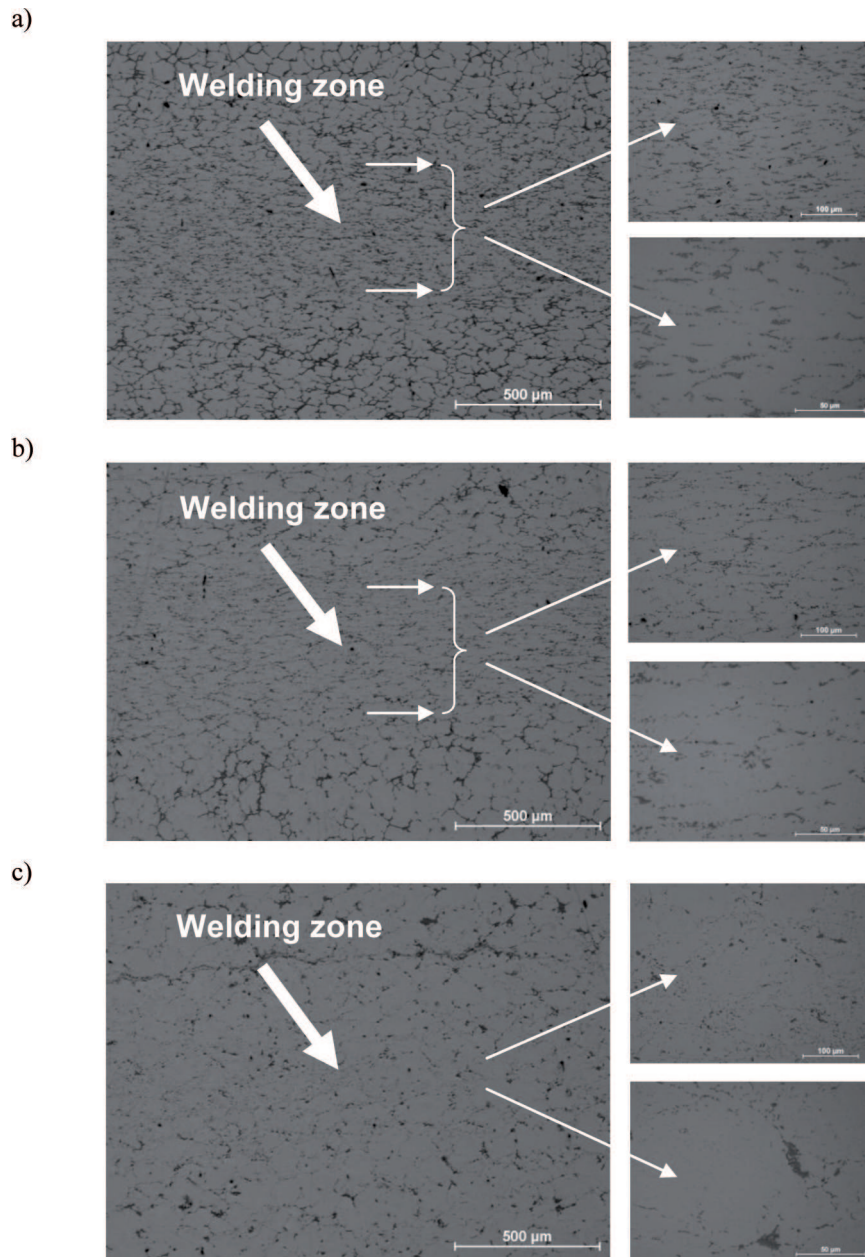


Fig. 7. Structures of the welded samples of alloy 2024 with the highest permissible content of Cu and Mg for different welding temperature (a)  $T = 430^{\circ}\text{C}$  (b)  $T = 500^{\circ}\text{C}$  (c)  $T = 530^{\circ}\text{C}$

In the case of the samples welded at  $430^{\circ}\text{C}$ , one observes a quite clear joining area (welding zone), which characterizes in a structure comminuted by plastic deformation, with small size particles (Figs 6a and 7a). It is estimated that the width of this area equals about 400 mm. The metal joining area is located between the areas practically not deformed, with the structure of equiaxial grains of relatively large sizes.

A similar structure of the welded samples, with a visible joining area, can be seen for a higher welding temperature ( $500^{\circ}\text{C}$ ), but only in regard to alloy 2024 with the highest permissible content of Cu and Mg (Fig. 7b). For the alloy with a minimized content of Cu

and Mg, we did not state a distinct welding area (Fig. 6b) – the material possesses an identical comminuted structure in the whole volume, with a lower number of particles and a lack of noticeable equiaxial grains (from the non-deformed area). Similar conclusions can be drawn for the samples with a minimized content of Cu and Mg, welded at  $530^{\circ}\text{C}$  (Fig. 6c), where a diversification of the structure between the welding area and the base material area (non-deformed) was not observed either. In the case of welding an alloy with a high content of the major alloying elements at  $530^{\circ}\text{C}$ , the metal joining area only slightly differs in the structural aspect from the base material (Fig. 7c).



Beside the structural tests, we examined the mechanical properties of 2024 alloy samples, welded at different temperatures and, for comparison, of non-welded samples, which were identically heated up to the same temperatures. We prepared suitable samples for hardness tests and tensile tests (round samples with the work diameter of  $D_0 = 2.5$  mm).

Fig. 8 presents the hardness HV values of the non-welded and the welded samples (for border contents of Cu and Mg) in the function of temperature. In the case of the welded samples, we showed the hardness both in the welding area (along the weld) and the base material area (non-deformed). We can see that at the given temperature, the hardness of the non-welded samples is almost the same as the hardness of the non-deformed ma-

terial in the welded samples. Generally, with the increase of temperature, the hardness HV increases as well, both for the welded and for the non-welded samples; however, the highest increase of hardness occurs in the temperature range of 430-500°C. A further raise of temperature results only in a slight increase of hardness.

In particular, for alloy 2024, both with a low and high content of Cu and Mg, slightly lower values of hardness were recorded for the welded samples (in the welding area), compared to the non-welded samples. Fig. 9 presents the ratio of the hardness HV of the welded samples to the hardness of the non-welded samples, in the functions of temperature and the content of Cu and Mg in the alloy.

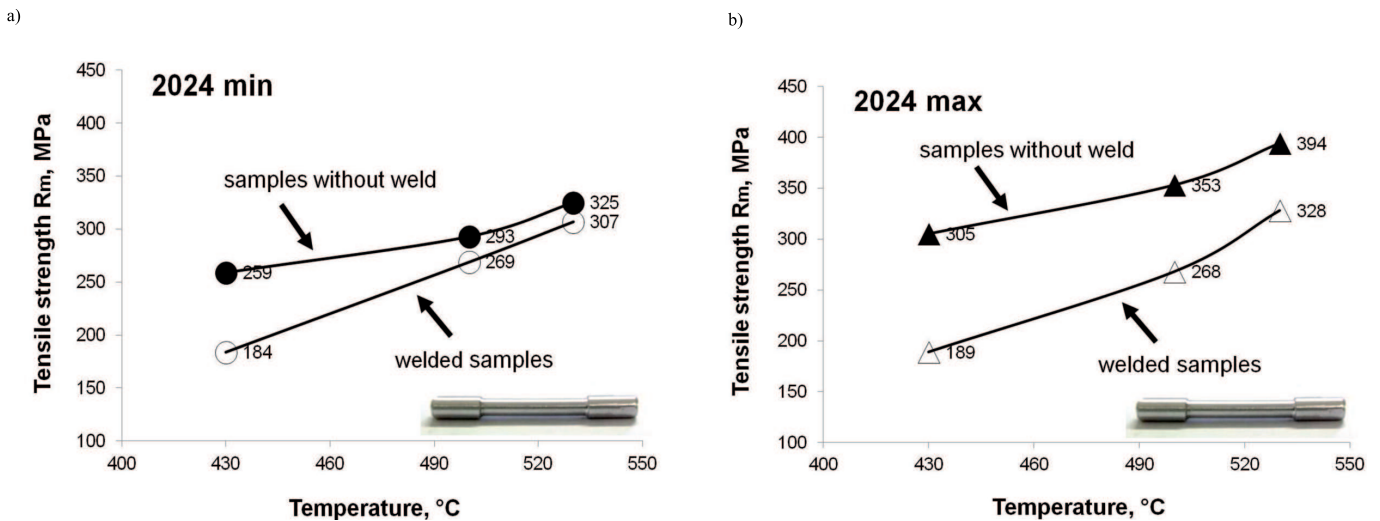


Fig. 8. Hardness HV of alloy 2024 with border contents of Cu and Mg (welded and non-welded samples) in the function of temperature (a) 2024 min, (b) 2024 max

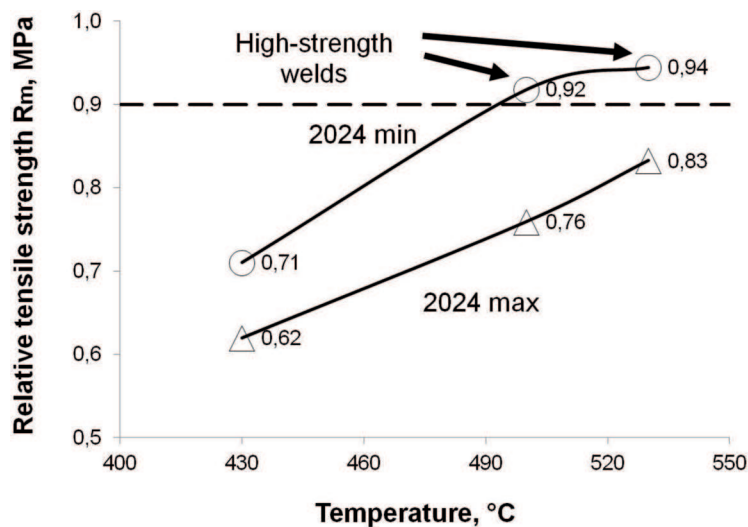


Fig. 9. Ratio of HV hardness of the welded samples to the hardness of the non-welded samples in the function of temperature (alloy 2024 with border Cu and Mg contents)



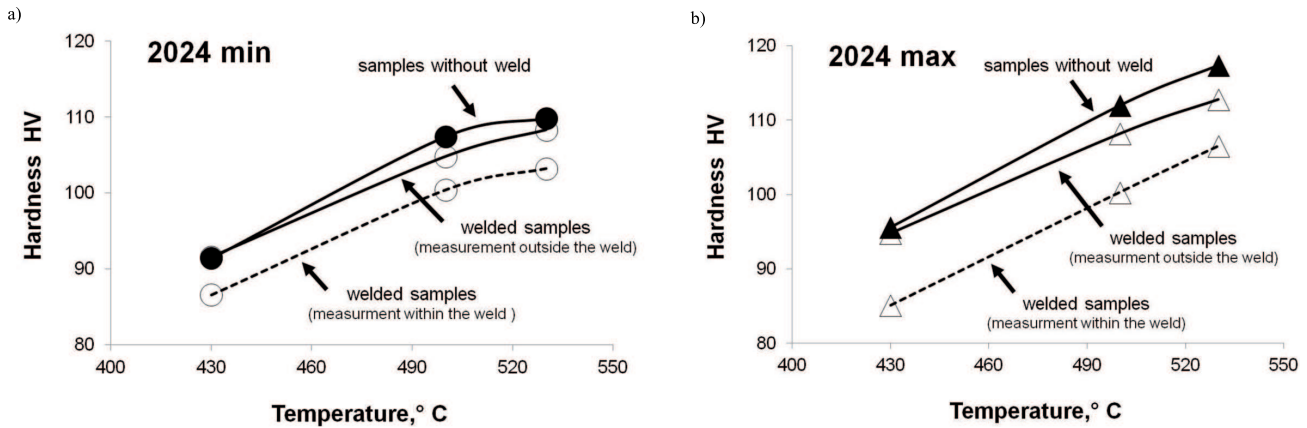


Fig. 10. Tensile strength  $R_m$  of alloy 2024 with border contents of Cu and Mg (welded and non-welded samples) in the function of temperature (a) 2024 min, (b) 2024 max

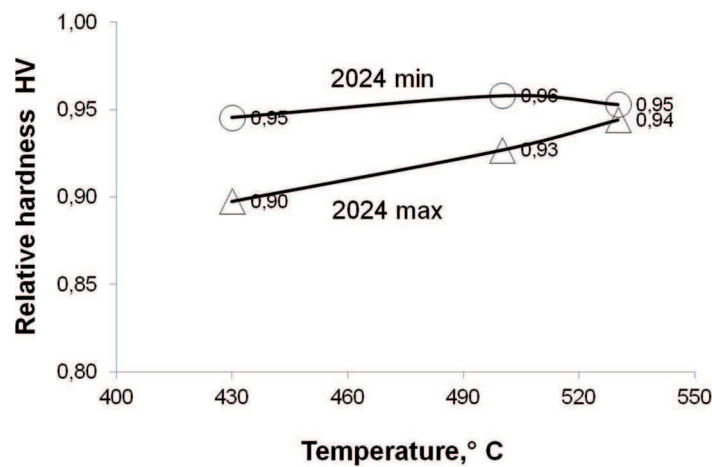


Fig. 11. Ratio of tensile strength  $R_m$  of the welded samples to the tensile strength of the non-welded samples in the function of temperature (alloy 2024 with border Cu and Mg contents)

We can notice that together with the rise of temperature, the hardness of the welded samples increases as well, referred to the analogous one, for the non-welded samples. At the same time, we can conclude that the rise of temperature decreases the effect of the Cu and Mg content in the alloy on the relative hardness of the welded samples and those without weld.

Fig. 10 shows the tensile strength  $R_m$  of alloy 2024 with the border contents of Cu and Mg (of the welded and non-welded samples), in the function of temperature. The rise of temperature increases the tensile strength  $R_m$  both for the welded and non-welded samples. At the same time, the values of tensile strength for the welded and non-welded samples become closer as temperature increases, which can be the evidence of improving conditions of welding. Fig. 11 presents the ratio of the tensile strength  $R_m$  of the welded samples to the analogous tensile strength of the non-welded samples, in the function of temperature (alloy 2024 with the border contents of Cu and Mg). In the diagram, the dashed

line designates the level of the tensile strength  $R_m$  of the welded samples, corresponding to 90% of the tensile strength  $R_m$  of the non-welded samples. For further considerations, it was assumed that the welds with their tensile strength exceeding that border are classified as high-strength welds. As is shown in Fig. 11, such welds can be obtained for alloy 2024 with a minimized content of Cu and Mg, at 500°C and 530°C; however, starting from the temperature 500°C up to 530°C, the weldability of the alloy improves only slightly. In the case of the alloy with the maximal content of Cu and Mg, even the application of the highest welding temperature (530°C) does not guarantee the obtaining a high strength weld (for the examined range of unit welding pressures).

## 6. Welding parameters

Figs. 12-13 present the stress parameters (mean stress  $\sigma_m$  and unit welding pressure  $p$ ) obtained in the

welding test of alloy 2024 with the border contents of Cu and Mg, in the function of the welding temperature. Generally, at the conditions of the performed welding tests, the rise of temperature leads to the increase of the mean stress (Fig. 12) and to an even greater increase of the unit welding pressure (Fig. 13). Slightly lower stress parameters were recorded for the alloy with a minimal content of Cu and Mg; however, with the increase of temperature, their values became closer.

Fig. 14 shows how the changing temperature affects the change in the ratio of the unit welding pressure  $p$  (obtained in the weldability tests) to the flow stress  $k$  of the examined alloy 2024 with the border contents of Cu and Mg. The higher the value of parameter  $p/k$ , the higher the potential weldability of the given material. In turn, when the unit welding pressure  $p$  reaches the border value of the minimal stress necessary to weld the given alloy  $\sigma_w$ , that is  $p = \sigma_w$ , then, the lower the value of parameter  $\sigma_w/k$ , the higher the weldability of the given material. At the lowest temperature 430°C, the values of parameter  $\sigma_w/k$  for alloy 2024 with a low and high content of Cu and Mg are relatively low (2.2 and 1.8, respectively). With such low values of parameter  $p/k$ , it is impossible to obtain high strength welds; however, minimizing Cu and Mg in alloy 2024 improves its weldability. Increasing the welding temperature to 500°C leads to an increase of parameter  $p/k$  up to 4.9, for a minimized chemical content of alloy 2024 and up to 4.1, for the alloy with the maximal content of Cu and Mg. As can be seen from the tests of the strength properties of the welds (Fig. 11), the value of parameter  $p/k$  equaling 4.9 is the border value for alloy 2024 with a minimized content of Cu and Mg, which means that the value of the minimal welding stress  $\sigma_w$  has been reached, guaranteeing the obtaining of a weld of a high tensile strength (weldability parameter  $\sigma_w/k = 4.9$ ).

A further increase of the welding temperature from 500°C to 530°C results in over a double increase of parameter  $p/k$  (11.5 and 9.5, respectively). However, even such a high value of this parameter for the alloy with the maximal content of Cu and Mg ( $p/k = 9.5$ ) does not ensure the obtaining of the minimal welding stress and, in consequence, does not allow for obtaining a high strength weld.

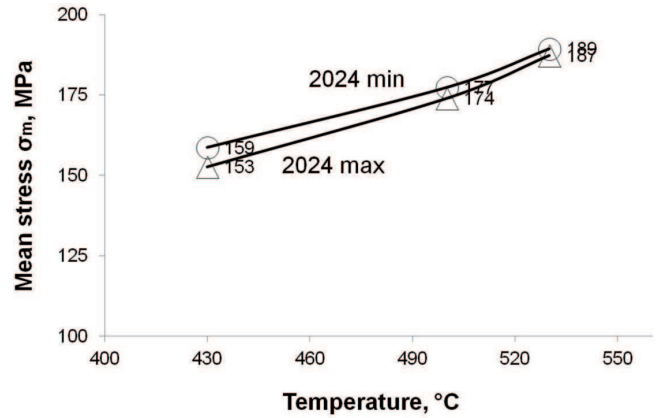


Fig. 12. Mean stress  $\sigma_m$  obtained in weldability tests of alloy 2024 with border Cu and Mg contents in the function of welding temperature

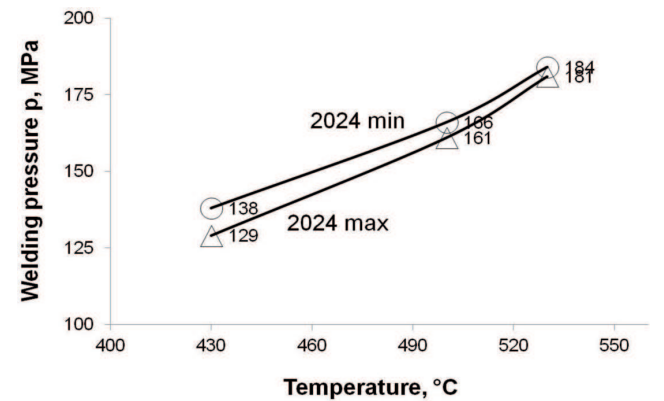


Fig. 13. Unit welding pressure  $p$  (normal compressive stress) in welding tests of alloy 2024 with border contents of Cu and Mg in the function of welding temperature

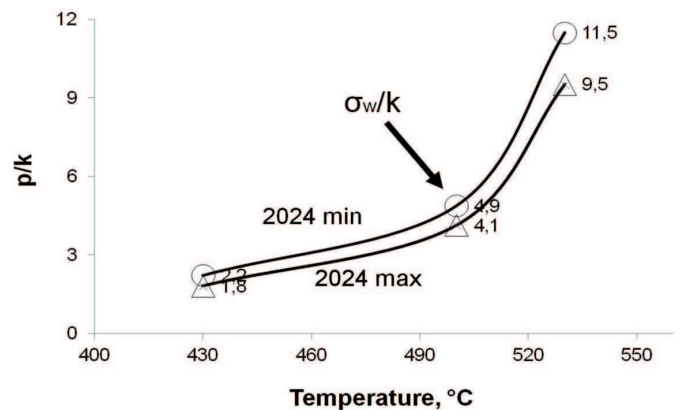


Fig. 14. Ratio of unit welding pressure  $p$  obtained in welding tests to flow stress  $k$  of alloy 2024 with border contents of Cu and Mg in the function of temperature

## 7. Conclusions

The paper proposed a method of weldability testing of aluminum alloys based on the principle of shearing

and welding of samples of the given alloy, at conditions imitating the parameters of the welding chamber of the porthole die.

By selecting suitable welding conditions for hard deformable and hard weldable AlCuMg alloys, one can influence the quality of the weld between the joined streams of metal. In particular, it is possible to determine precise values of the minimal welding stress  $\sigma_w$  for alloy 2024, which guarantee the obtaining of a joint of metal and high strength weld. A minimization of the Cu and Mg contents in the examined alloy, together with the application of the welding temperature equaling 500°C, make it possible to obtain a high strength weld, with the minimal welding stress  $\sigma_w$  at the level of 166 MPa. We defined the parameter describing the ability of a material to weld ( $\sigma_w/k$ ), which also includes the value of the flow stress  $k$  of the welded material, dependent on temperature. We determined the value of that parameter for alloy 2024, with a minimized content of Cu and Mg, welded at 500°C ( $\sigma_w/k = 4.9$ ). This means that a high strength weld in this alloy can be obtained when the value of the compressive stress is almost five times larger than the value of the flow stress. In the case of alloy 2024 with the maximal content of Cu and Mg, even the application of the welding temperature equaling 530°C and the level of compressive stresses almost ten times larger than the value of the flow stress, do not provide for a high strength weld. Generally, the larger content of Cu and Mg in the alloy, the lower weldability and the higher should be the welding temperature and the ratio of the unit welding pressure to the flow stress ( $p/k$ ). It can, however, turn out that, for the alloys with a high content of Cu and Mg, obtaining in practice suitable values of welding parameters will be exceptionally difficult or even impossible. The values of the minimal welding stress for alloy 2024 obtained in the weldability tests are the basis for the designing of porthole dies, and especially welding chambers with an optimal shape and dimensions, which, during extrusion at a given temperature, will be able to generate similar compressive stresses to those determined by the invented method.

The method and the device for weldability tests can have their industrial application mainly in the designing of technologies for extrusion through porthole dies of tubes and various hollow sections from aluminum and its

alloys, especially those hard deformable and hard weldable ones. The invention makes it possible to determine the optimal temperatures of extrusion and the extrusion rates of particular types of alloys. It is helpful in designing of the welding chambers of porthole die.

#### REFERENCES

- [1] R.F. Tylecote, The solid phase welding of metals, Edward Arnold Publishers Ltd., London, 1968.
- [2] L. Kowalczyk, Łączenie metali w stanie stałym w procesach obróbki plastycznej, Warszawa, 1988.
- [3] J. Zasadziński, W. Libura, J. Richert, Prędkość wypływu trudnoodkształcalnych stopów Al podczas wyciskania w temperaturach bliskich temperatury topnienia, Rudy Metale **50**, 12, 686-689 (2005).
- [4] D. Leśniak, M. Bronicki, A. Woźnicki, High-temperature homogenization of AlCuMg alloys for extrusion in T5 temper. Archives of Metallurgy and Materials **55**, 2, 499-513 (2010).
- [5] J. Wantuchowski, J. Zasadziński, J. Richert, Badania nad zastosowaniem matryc mostkowych w praktyce wyciskania na gorąco aluminium i jego stopów, Zeszyty Naukowe AGH, z. 59, 259-274 (1974).
- [6] J. Zasadziński, J. Richert, W. Misiołek, Weld Quality in Extruded Aluminum Hollow Section, Light Metal Age **51**, 4, 8-13 (1993).
- [7] R. Akeret, Properties of pressure welds in extruded aluminum alloy sections, Journal of the Institute of Metals **100**, 202-207 (1972).
- [8] Szczegoliewatych i in.: Isljedowanie wlijanja dawljenja na procznost szwow, poluczennych priessowoj swarkoj, Cwietnyje Mietalły, nr 11, 66-71, 1970.
- [9] Patent USA, Welding of Aluminium and Magnesium Alloy, nr 40787, 1978.
- [10] J. Zasadziński, J. Richert, W. Libura, M. Galanty, D. Leśniak, A. Rękas, Dobór warunków zgrzewania trudno odkształcalnych stopów aluminium przeznaczonych do wyciskania kształowników na matrycach mostkowo-komorowych, Rudy i Metale **54**, 3, 148-152 (2009).
- [11] J. Richert, J. Zasadziński, W. Libura, M. Galanty, D. Leśniak, A. Rękas, Method and the device for weldability testing of metals and alloys, preferably aluminum alloys intended for extrusion on the porthole dies, Polish Patent nr P-390 383, 2010.